Available online at www.sciencedirect.com
SCIENCE DIRECT®
Thermochimica Acta 426 (2005) 131–139
thermochimica acta
www.elsevier.com/locate/tca

Studies on energetic compounds Part 31. Thermolysis and kinetics of RDX and some of its plastic bonded explosives

Gurdip Singh[a,*], S. Prem Felix[a], Pramod Soni[b]

[a] *Department of Chemistry, DDU Gorakhpur University, Gorakhpur 273009, India*
[b] *Terminal Ballistic Research Laboratory, Chandigarh 160020, India*

Received 7 January 2003; received in revised form 22 July 2004; accepted 22 July 2004
Available online 11 September 2004

Abstract

Thermal analysis of RDX and its three plastic bonded explosives (PBXs) namely RXE 9505, RXE 9010 and RXV 9010 were done using various thermo analytical techniques, under different conditions. Although, the thermal analyses do not show any significant reduction in thermal stability of RDX, there are results, which suggest that the presence of binder alters the reaction pathways. Kinetic analysis of isothermal TG data was made by model fitting methods as well as a model free isoconversional method. The merits and demerits of both modes of kinetic approaches were evaluated critically. Conventional model fitting methods fail to describe the complex reactions during thermolysis of both RDX and its PBXs. Isoconversional method shows that the mechanisms of thermolysis of RDX and its PBXs are different, in the same temperature range. Role of binder was found to be in facilitating the reaction to take place in the condensed phase and reducing the role of competing reaction channels such as evaporation and gas phase thermolysis. Rapid thermolysis of the samples was studied by measuring ignition delay and evaluating its kinetic parameters.

Keywords: Plastic bonded explosives; RDX; Thermolysis; Kinetics; Isoconversional method

1. Introduction

PBX is a composite energetic material (CEM), which contains an energetic compound as filler in a polymer (binder) matrix. The basic aim of coating an energetic compound with a polymer binder is to reduce its sensitivity and give mechanical strength for shaped explosive charges. Pressing is made easier in PBX moulding powders and thus the higher density helps to attain better performance. Thermal analysis is an integral part of research and development of high energetic materials (HEMs) due to obvious reasons. Initiation by most of the hazardous stimuli such as shock, impact, spark, etc., is believed to be triggered off by the thermal event produced [1]. Moreover, thermal decomposition mechanisms and products influence the performance of HEMs. Thus deep understanding of various physico-chemical processes that are occurring during thermolysis of HEMs is required for performance prediction and safety evaluation.

Thermal behavior of PBXs may be different from that of pure energetic compound because the binder as well as other additives such as plasticiser may influence the thermo chemistry. In fact studies on composite solid propellants, which are essentially similar in composition to that of PBXs show that binder plays a vital role in their thermolysis and combustion. For example, Oyumi et al. [2] showed that presence of bis(azidomethyl)oxetane/tetrahydrofuran (BAMO), which is a copolymer binder, initiated and accelerated the rate of HMX thermal decomposition in their composite propellant. Bazaki et al. [3] have investigated the effect of chemical nature of binder on burning rate characteristics of ammonium perchlorate (AP) based composite propellants. They have concluded

* Corresponding author. Tel.: +91 551 2202856; fax: +91 551 2340459.
E-mail address: gsingh4us@yahoo.com (G. Singh).

0040-6031/$ – see front matter © 2004 Elsevier B.V. All rights reserved.
doi:10.1016/j.tca.2004.07.013

that burning rate appears to be very much dependent on the type of binder used. However, the role of binder in thermolysis of PBXs is less explored [4] and meagerly available in open literature. Various establishments involved in formulation of PBXs have reported some routine characterization of PBXs [5–9]. But these are inadequate to understand the effect of binder on thermal stability of the energetic filler and the underlying thermo chemistry. Thus, some systematic thermal studies on various PBX formulations have been initiated in this laboratory. Thermal analysis and kinetics thereof on RDX–HTPB PBX, showed that the thermolysis pathways are different in pure RDX and the PBX [4,10]. Our recent studies [11] showed that thermal stability of HMX decreases when it is coated with Estane and extent of lowering increases as the percentage of binder increases. Thus, it was found interesting to study the role of Estane during thermolysis of its PBX with RDX. The effect of Viton A, which is thermally more stable than Estane has also been investigated and the results are presented here.

There are a number of correlations available in literature between kinetics of thermolysis in HEMs and performance parameters. Cook et al. [12,13] proposed that the kinetics of initial reactions are important in determining detonation velocity. Zeman et al. correlated thermal decomposition kinetics of polynitroaromatic explosives at lower temperature with molecular structure [14], heat of explosion [15], detonation characteristics [14,16], and thermal stability [17]. The Arrhenius parameters are related to critical temperature of thermal explosion by Frank-Kamenetski model [18]. Thus it is important to assess the kinetic parameters for thermolysis of HEMs. Traditionally, model-fitting [19,20] approaches are used for evaluating global activation energy and pre-exponential factor. However, thermolysis of energetic materials is highly complex and is an intricate interplay of various physicochemical processes. The individual steps may have different activation energies and contribution of individual steps to overall process may be a function of both temperature as well as extent of conversion. Such changes are not detected by traditional model fitting methods [21,22]. Recently the use of isoconversional methods is suggested as a solution for this problem [23,24]. We have used both traditional methods as well as a standard isoconversional method [25], for evaluating kinetic parameters for isothermal TG data of RDX and its PBXs. The Arrhenius parameters obtained using both methods have been compared critically.

2. Experimental section

Samples of RDX, Estane, Viton A and their PBX formulations containing RDX and Estane in the ratios 95:5 (RXE 9505), 90:10 (RXE 9010) and a RDX-Viton A PBX in the ratio 90:10 (RXV 9010) were supplied by TBRL, Chandigarh. These samples were used as received. Non-isothermal TG-DTG analyses of the samples were done by using a DuPont 2100 TG instrument at a heating rate of 10 °C min^{-1} (sample mass ≈5 mg, atmosphere = flowing N_2 gas at a rate of 60 mL min^{-1}). DSC thermal curves on the samples in open aluminium pans were collected by using DuPont 2100 DSC instrument at a heating rate of 10 °C min^{-1} (sample mass ≈2 mg, atmosphere = flowing N_2 gas at a rate of 60 mL min^{-1}). Non-isothermal TG-DSC analyses on the samples were made on NETZSCH STA 409 at a heating rate of 10 °C min^{-1} under flowing N_2 (60 mL min^{-1}) in an alumina crucible with a lid having small (pin size) hole in the centre. Non-isothermal TG analyses were also made in static air atmosphere at a heating rate of 10 °C min^{-1}, using an indigenously fabricated TG apparatus [26] (sample mass ≈25 mg). DTA analyses of the samples were carried out in flowing air (60 mL min^{-1}) atmosphere at a heating rate of 10 °C min^{-1}, using a DTA apparatus by Universal Thermal Analysis Instruments, Mumbai. Sample mass was kept as ∼5 mg for RDX and the PBXs. Isothermal TG studies of the samples were done at appropriate temperatures using the above stated indigenously fabricated TG apparatus under static air atmosphere. Approximately 25 mg sample mass has been used for each run. Measurements of ignition delay of RDX and the PBXs were made by tube furnace technique (TF) [27]. Details of the experiments were as reported earlier [28]. Thus all the experiments were in open condition, except in STA, where the analyses were made under partial confinement.

3. Results

3.1. TG-DTG and DSC

TG-DTG thermal curves of RDX, RXE 9505, RXE 9010, RXV 9010 and Viton A are given in Fig. 1 and the phenomenological data are summarized in Table 1. TG thermal curve of RDX exhibits mass loss in a single step, which approaches ∼100%. Mass loss in Viton A takes place at very high temperature and its thermolysis occurs in a single step. TG and DSC thermal curves for pure Estane are not included, they are reported in our earlier paper [11]. TG-DTG thermal curves for PBXs differ from that of pure RDX in that there is an additional step of binder degradation, which follows the thermolysis of RDX in the first step. The second step in the case of Estane based PBXs is occurring in a wide range of temperatures. However, the second step for RXV 9010 is clearly distinct and the values of T_i, inflection temperature (T_s) and end-set temperature (T_f) for this step are given in Table 1.

DSC thermal curves are shown in Fig. 2 and the corresponding data are summarized in Table 1. Fig. 2 shows an endotherm followed by an exotherm for RDX and its PBXs. The initial sharp endothermic peak at ∼206 °C is due to melting of RDX [29]. Enthalpy change (ΔH) during the exothermic decomposition of RDX and its PBXs is also calculated and given in Table 1. DSC thermal curve for Viton A does not show any process up to 400 °C, which is the upper tempera-

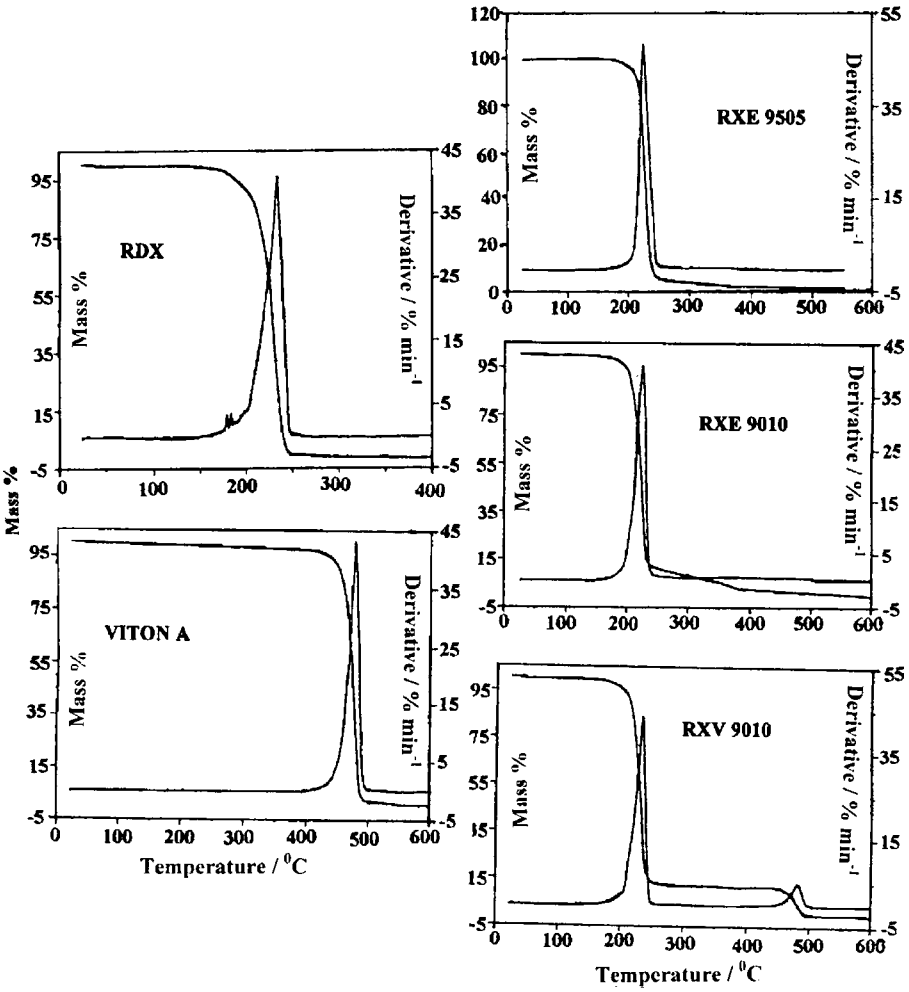

Fig. 1. TG-DTG thermal curves of RDX, Viton A and their PBXs in inert atmosphere.

ture limit of the instrument. Hence the corresponding thermal curve is not included in Fig. 2.

3.2. Simultaneous TG-DSC

Thermal curves recorded by STA in the temperature range of 100–350 °C are shown in Fig. 3 and the data are summarized in Table 2. T_i, T_s and T_f for all samples in TG were found to have a higher value than that obtained in open conditions. The peak temperature in DSC was also higher for all samples than that obtained in open pans. From the overlay of TG thermal curves in Fig. 3, it can also be seen that mass loss in RDX and RXE 9505 starts even before T_i. But, as the percentage of binder increases, there is no significant mass loss prior to T_i.

3.3. Non-isothermal TG and DTA in static air

Non-isothermal TG experiments were carried out in static air atmosphere to determine the range of temperature for

Table 1
TG-DTG and DSC phenomenological data of RDX and its PBXs under inert atmosphere in open pans

Sample name		TG-DTG				DSC peak temperature (°C), Exo	ΔH (kJ g^{-1}), Exo
		T_i (°C)	T_s (°C)	T_f (°C)	% Decomposition		
RDX		216	232	240	99.7	236, 249[a]	0.54
RXE 9505		214	224	235	96.7	239	1.2
RXE 9010		212	226	234	92.4	240	1.4
RXV 9010	I	219	232	239	87.1	240	1.2
	II	467	481	489	11.8	–	–
Viton A		462	477	485	97.8	–	–

T_i: onset temperature; T_s: inflection temperature; T_f: end-set temperature.
[a] Shoulder peak.

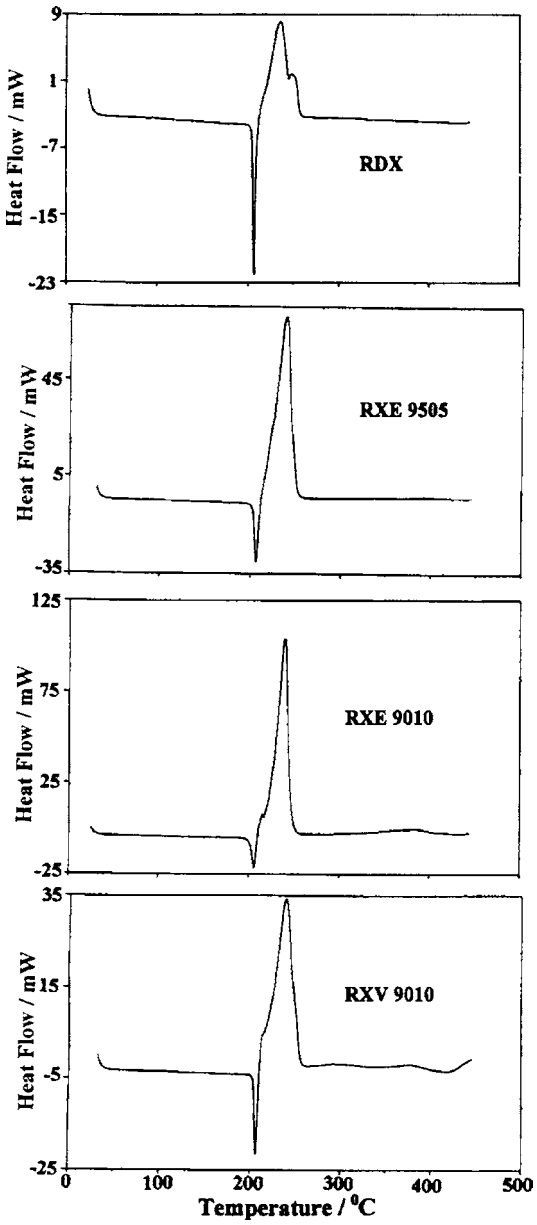

Fig. 2. DSC thermal curves of RDX and its PBXs in open pans.

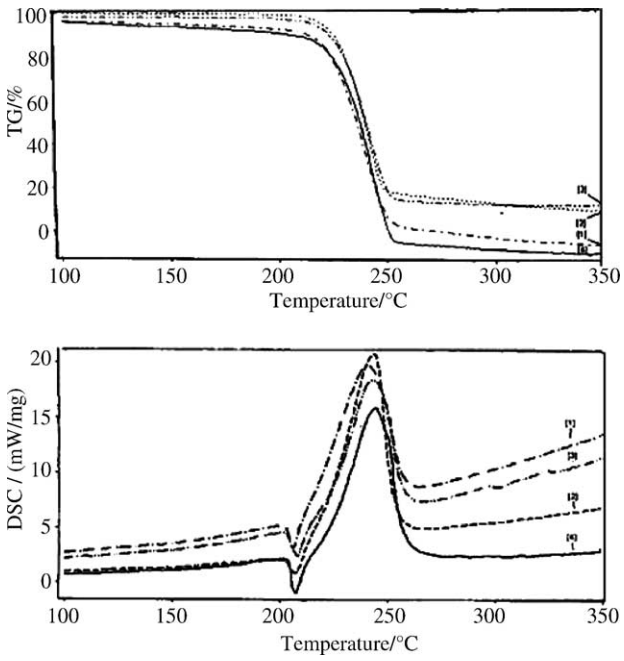

Fig. 3. Simultaneous TG-DSC thermal curves of RDX [4], RXE 9505 [1], RXE 9010 [2] and RXV 9010 [3] under inert atmosphere, in a pan having a lid with hole (small pin sized) at the centre.

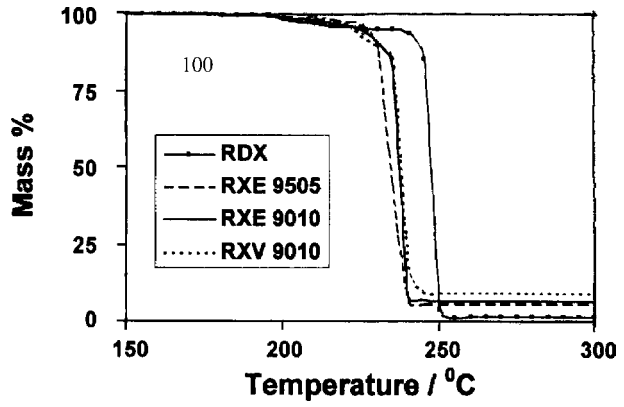

Fig. 4. Non-isothermal TG thermal curves of RDX and its PBXs in static air atmosphere.

conducting isothermal analysis under similar conditions. TG thermal curves are shown in Fig. 4 and the data profiles are summarized in Table 3. The DTA thermal curves are shown in Fig. 5 and the corresponding data are given in Table 3. TG thermal curves show that although the starting decomposition temperature (SDT) is same for RDX and its PBXs, thermolysis completes earlier in case of PBXs. Nature of the DTA thermal curves is more or less similar to that of the DSC ones.

Table 2
Simultaneous TG-DTG–DSC phenomenological data of RDX and its PBXs in inert atmosphere and partial confinement of samples

Sample name	TG-DTG				DSC peak temperature (°C), Exo	ΔH (kJ g^{-1}), Exo
	T_i (°C)	T_s (°C)	T_f (°C)	% Decomposition		
RDX	220	242	255	98.4	244	1.0
RXE 9505	218	238	254	92.2	240	1.7
RXE 9010	219	241	250	84.1	244	1.8
RXV 9010	224	241	255	83.3	243	1.5

T_i: onset temperature; T_s: inflection temperature; T_f: end-set temperature.

Table 3
TG and DTA phenomenological data of RDX and its PBXs in static air atmosphere

Sample name	TG			DTA peak temperature (°C)	
	SDT (°C)	FDT (°C)	% Decomposed	Endo	Exo
RDX	200	250	99	207	246
RXE 9505	200	240	96	206	244
RXE 9010	201	242	93	207	248
RXV 9010	202	240	90	207	246

SDT: starting decomposition temperature; FDT: final decomposition temperature.

3.4. Isothermal TG

Plot of data derived from isothermal TG for RDX, RXE 9505, RXE 9010 and RXV 9010 are given in Fig. 6. Temperature range chosen was above the melting point of RDX in all cases. For RDX, isothermal TG analysis was possible even at a temperature as high as 240 °C, whereas the PBXs were found to decompose faster at this temperature leading to runaway reactions. Shape of the thermal curves for all samples was sigmoidal, which is usually attributed to autocatalytic reactions.

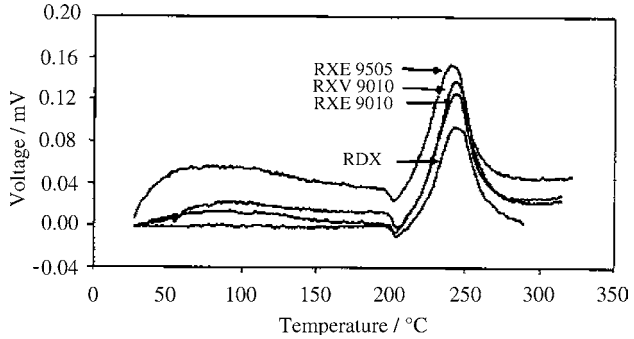

Fig. 5. DTA thermal curves of RDX and its PBXs in static air atmosphere.

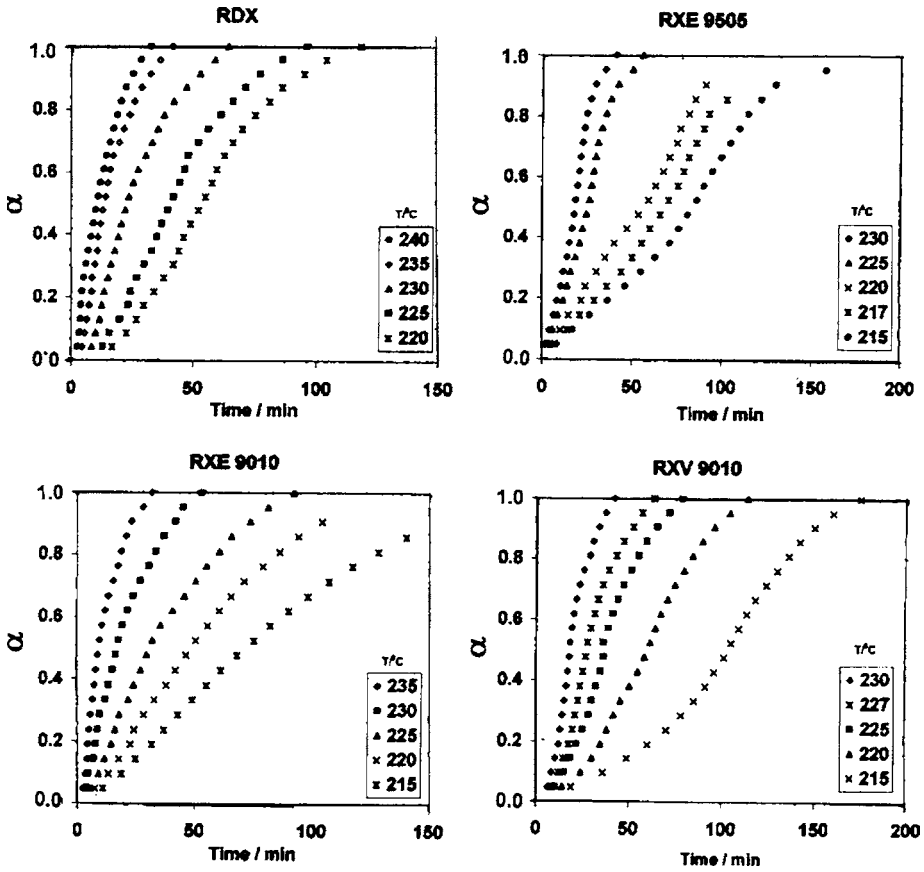

Fig. 6. Plot of α vs. time of RDX and its PBXs in static air atmosphere.

Table 4
Various mechanism based kinetic models generally used to describe thermal decomposition of solids

S. no.	Model	$f(\alpha)$	$g(\alpha)$
1.	Power law	$4\alpha^{3/4}$	$\alpha_{1/4}$
2.	Power law	$3\alpha^{2/3}$	$\alpha^{1/3}$
3.	Power law	$2\alpha^{1/2}$	$\alpha^{1/2}$
4.	POWER law	$2/3\alpha^{-1/2}$	$\alpha^{3/2}$
5.	One-dimensional diffusion	$1/2\alpha^{-1}$	α^2
6.	Mampel (first order)	$1-\alpha$	$-\ln(1-\alpha)$
7.	Avrami–Erofeev	$4(1-\alpha)[-\ln(1-\alpha)]^{3/4}$	$[-\ln(1-\alpha)]^{1/4}$
8.	Avrami–Erofeev	$3(1-\alpha)[-\ln(1-\alpha)]^{2/3}$	$[-\ln(1-\alpha)]^{1/3}$
9.	Avrami–Erofeev	$2(1-\alpha)[-\ln(1-\alpha)]^{1/2}$	$[-\ln(1-\alpha)]^{1/2}$
10.	Contracting sphere	$3(1-\alpha)^{2/3}$	$1-(1-\alpha)^{1/3}$
11.	Three-dimensional diffusion	$2(1-\alpha)^{2/3}(1-(1-\alpha)^{1/3})^{-1}$	$[1-(1-\alpha)^{1/3}]^2$
12.	Contracting cylinder	$2(1-\alpha)^{1/2}$	$1-(1-\alpha)^{1/2}$
13.	Prout–Tomkins	$\alpha(1-\alpha)$	$\ln(\alpha/1-\alpha)$
14.	Ginstling–Brounshtein	$3/2[(1-\alpha)^{-1/3}-1]^{-1}$	$[1-(2\alpha/3)]-(1-\alpha)^{2/3}$

3.5. Kinetic analysis of isothermal TG data

3.5.1. Model fitting methods

The equation generally used for kinetic evaluation of thermal decomposition reactions is the well-known expression for rate, which is

$$\frac{\mathrm{d}a}{\mathrm{d}t} = k(T)f(\alpha) \tag{1}$$

where α is the extent of conversion, t the time, T the absolute temperature, $k(T)$ the temperature-dependent rate constant and $f(\alpha)$ a function called the reaction model. Various forms of $f(\alpha)$ are summarized in Table 4. The temperature dependency of rate constant is assumed to obey Arrhenius expression:

$$k(T) = A\ \exp\left(-\frac{E}{RT}\right) \tag{2}$$

where A is pre-exponential (Arrhenius) factor, E the activation energy and R the gas constant. Eq. (1) is often used in its integral form, which for isothermal conditions becomes:

$$g(\alpha) \equiv \int_0^\alpha [f(\alpha)]^{-1}\,\mathrm{d}\alpha = k(T)t \tag{3}$$

where $g(\alpha)$ is integrated form of the reaction model (Table 3). Substituting a particular reaction model into Eq. (3) results in evaluating the corresponding rate constant, which is found from slope of the plot of $g(\alpha)$ versus t. For each reaction model selected, the rate constants are evaluated at several temperatures and the Arrhenius parameters are evaluated using Arrhenius equation in its logarithmic form:

$$\ln\ k(T) = \ln\ A - \frac{E}{RT} \tag{4}$$

Kinetic parameters obtained for isothermal decomposition of RDX, RXE 9505, RXE 9010 and RXV 9010 are given in Tables 5–8, respectively. The correlation coefficient (r) is sometimes used as a parameter for choosing the best model. The values of r are also reported in Tables 5–8.

Table 5
Arrhenius parameters for isothermal decomposition of RDX

Model[a]	E (kJ mol^{-1})	ln(A) (min^{-1})	r
1	151.1	31.4	0.9918
2	152.0	31.8	0.9916
3	153.7	32.5	0.9913
4	160.8	34.5	0.9892
5	162.8	35.0	0.9883
6	159.2	35.2	0.9892
7	154.8	32.8	0.9908
8	155.6	33.3	0.9905
9	157.0	34.0	0.9901
10	159.6	33.7	0.9893
11	160.7	33.5	0.9883
12	159.4	33.9	0.9895
13	154.0	34.5	0.9908
14	162.2	33.4	0.9880

[a] Enumeration of the model is as given in Table 4.

3.5.2. Isoconversional method

In isoconversional method, it is assumed that the reaction model in Eq. (1) is not dependent on temperature. Under isothermal conditions, we may combine Eqs. (3) and (4) to

Table 6
Arrhenius parameters for isothermal decomposition of RXE 9505

Model[a]	E (kJ mol^{-1})	ln(A) (min^{-1})	r
1	217.4	47.9	0.9860
2	217.5	48.1	0.9860
3	217.7	48.4	0.9860
4	219.1	49.0	0.9855
5	219.8	49.1	0.9850
6	221.3	50.5	0.9825
7	218.8	48.7	0.9848
8	219.1	49.0	0.9846
9	219.6	49.5	0.9842
10	220.1	48.7	0.9840
11	222.6	48.7	0.9810
12	219.6	48.8	0.9847
13	219.2	50.7	0.9842
14	221.5	48.0	0.9828

[a] Enumeration of the model is as given in Table 4.

Table 7
Arrhenius parameters for isothermal decomposition of RXE 9010

Model[a]	E (kJ mol^{-1})	ln(A) (min^{-1})	r
1	184.3	39.5	0.9932
2	184.7	39.8	0.9932
3	185.5	40.2	0.9931
4	189.1	41.4	0.9927
5	190.5	41.8	0.9926
6	192.0	43.1	0.9922
7	187.5	40.8	0.9928
8	188.0	41.2	0.9928
9	189.1	41.8	0.9926
10	190.4	41.2	0.9925
11	194.0	41.6	0.9924
12	189.6	41.3	0.9926
13	187.9	42.8	0.9928
14	192.7	40.8	0.9923

[a] Enumeration of the model is as given in Table 4.

Table 8
Arrhenius parameters for isothermal decomposition of RXV 9010

Model[a]	E (kJ mol^{-1})	ln(A) (min^{-1})	r
1	187.2	40.5	0.9878
2	188.3	41.0	0.9880
3	190.6	41.7	0.9885
4	202.0	44.8	0.9907
5	206.5	45.9	0.9914
6	210.8	47.9	0.9920
7	196.3	43.2	0.9896
8	198.1	43.9	0.9899
9	201.6	45.1	0.9906
10	205.8	45.2	0.9913
11	217.6	47.5	0.9930
12	203.3	44.8	0.9909
13	197.4	45.3	0.9898
14	213.5	46.1	0.9924

[a] Enumeration of the model is as given in Table 4.

get

$$-\ln t_{\alpha,i} = \ln\left[\frac{A}{g(\alpha)}\right] - \frac{E_\alpha}{RT_i} \quad (5)$$

where E_α is evaluated from slope for the plot of $-\ln t_{\alpha,i}$ against T_i^{-1}. Thus values of E_α for RDX and PBXs were evaluated at various α_i. The dependencies of activation energy (E_α) on extent of conversion (α) are given in Fig. 7.

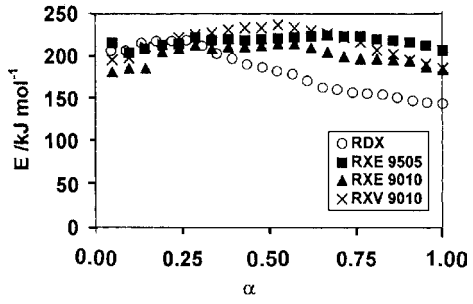

Fig. 7. Dependencies of activation energy on extent of conversion for RDX and its PBXs obtained using the isoconversional method.

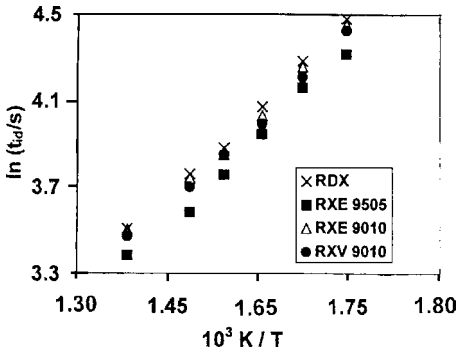

Fig. 8. Plot of ln(t_{id}) against T^{-1} for RDX and its PBXs.

3.6. Ignition delay (t_{id}) studies

Measurement of t_{id} at various temperatures for RDX and the PBXs was done and the values are summarized in Table 9. The values of t_{id} fitted the following equation [30–32]:

$$t_{id} = A \exp\frac{E^*}{RT} \quad (6)$$

where E^* is the activation energy for thermal ignition. Eq. (6) is used in its logarithmic form to evaluate E^* from a plot of $\ln t_{id}$ against T^{-1}. The plot of $\ln t_{id}$ against T^{-1} for RDX and its PBXs are given in Fig. 8 and the values of E^* are summarized in Table 9.

4. Discussion

Thermolysis of RDX involves reactions in many phases and hence the use of open and confined pans for analyses using TG and DSC, allows to vary the contributions of condensed and gas phase processes [33,34]. Results of thermal analyses at various conditions and using different techniques do not indicate any considerable reduction in the thermal stability of RDX in its PBXs. Moreover, thermal analysis shows that thermolysis of RDX and its PBXs have similar T_i values. But, non-isothermal TGA under static air atmosphere shows that thermolysis of PBXs completes earlier as compared to RDX. Isothermal TGA shows that thermolysis of RDX is slower at higher temperatures where that of PBXs occurs quite faster.

Value of ΔH for the exothermic process for RDX as per DSC in open pans and in pierced pans is less than that of its PBX analogues. Thus, it may be seen that coating with a binder favours exothermic decomposition of RDX. Recently Long et al. [34] have studied the competitive vaporization and decomposition of liquid RDX. They have shown that confining an RDX sample in a closed pan prevents sublimation of solid RDX and size of the normalized exotherm increases as compared to that observed in open pan experiments. Thus, it seems that the polymeric binder might be forming a superficial layer over molten RDX, which prevents evaporation and thus thermolysis proceeds in the liquid phase. Exothermic

Table 9
Ignition delay (t_{id}) and activation energy for thermal ignition (E^*) for RDX and its PBXs

Sample	t_{id} (s) at temperatures (°C)						E^* (kJ mol^{-1})	r
	300	325	350	375	400	450		
RDX	88.13	72.50	58.75	48.53	42.92	33.28	22.6	0.9982
RXE 9505	74.66	64.03	51.78	42.62	35.97	29.37	22.4	0.9962
RXE 9010	85.50	70.47	56.44	47.07	42.18	33.12	22.1	0.9966
RXV 9010	83.25	67.25	54.45	46.97	40.5	32.12	22.0	0.9978

heat release is more prevalent in Estane based PBXs than the Viton A formulation. It was observed in our earlier study [11] that depolycondensation of urethane linkage in Estane takes place, regenerating the diol and the isocyanate at ∼223 °C. Thus liquid oligomers can provide better cover than Viton A, which is a thermally stable polymer.

TG-DTG thermal curve in Fig. 1 for RXV 9010 has a clearly distinct second step of binder decomposition. It is evident from Table 1 that there is 87.1% mass loss in the first step. As mass loss for pure RDX sample is ∼100%, it may be inferred that actual mass% of binder in RXV 9010 is slightly more than 10%. For the Estane PBXs, % mass loss in the first step is higher than the theoretical mass loss for RDX decomposition. This may be due to the gasification of Estane, caused by the higher condensed phase heat release in its PBXs combined with open condition. Such a result has been observed in our earlier study [11] on HMX-Estane PBXs. But in confined pan TG experiments, mass loss in the first step for PBXs is lower (Table 2) than even the theoretical mass loss of RDX. The partial confinement might have prevented gasification of the binder in Estane PBXs.

4.1. Kinetic analysis

Values of r reported in Tables 5–8 are very close to each other, so that choosing 'best fit' based on them is not possible. Values of activation energy are close to each other for a sample irrespective of the equation used. Thus for RDX, RXE 9505, RXE 9010 and RXV 9010, an average value of ∼157, ∼220, ∼189 and ∼201 kJ mol^{-1} was obtained as activation energy respectively. Kishore [33] has reported that an activation energy of 171 ± 8 kJ mol^{-1} may be considered as the authentic value, for thermolysis of RDX. Thus our estimate of ∼157 kJ mol^{-1} is a good one. But most of the studies in melt phase of RDX reported [2,35–38] a value of ∼200 kJ mol^{-1}. Brill et al. [39] have compiled the values of kinetic parameters reported in literature and found that all these E and ln A values usually compensate for one another. They have argued that all the E, ln A pairs, which lie in the regression line of their kinetic compensation plot are valid and correct for the specific characteristics of the sample and measurement used. We have plotted all the values of E for RDX and its PBXs, reported in Tables 5–8 against corresponding ln A values and is shown in Fig. 9. It can be seen from the plot that all values fall in a straight line and obey the following equation:

$$\ln A = a + bE \quad (7)$$

These kinetic parameters suffer from kinetic compensation effect. Further, as per the arguments of Brill et al. [39], variation of E for the PBXs from RDX is only due to the change in sample characteristics, since our experimental conditions are the same. So it is not clear whether there is any change in mechanism for thermolysis of RDX in its PBXs, from the kinetic parameters obtained using conventional model fitting methods. Moreover, the mechanism of thermolysis of RDX is not so simple to be defined by a single value of kinetic parameters [34].

The conventional model fitting approach fails to reveal the complexities during thermolysis. The model free isoconversional method has been recently applied [34] to study the kinetics of thermolysis of liquid RDX using non-isothermal TG and DSC techniques. Hence it was thought appropriate to use the same method for kinetic analysis of isothermal TG data of RDX and its PBXs. Fig. 7 shows that the activation energy for RDX changes from an initial value of 200 kJ mol^{-1} up to $\alpha = 0.25$ to ∼150 kJ mol^{-1} at higher values of α. Long et al. [34] have explained such a variation in activation energy. The liquid state thermal decomposition of RDX is occurring through three major steps: vaporization, liquid phase decomposition and gas phase decomposition, which are having activation energies of ∼100, ∼200 and ∼140 kJ mol^{-1}, respectively. Thus initial stages of isothermal decomposition of RDX are dominated by liquid phase decomposition. But, contribution from the other two competing channels increases as the reaction progresses and hence the reduction in activation energy.

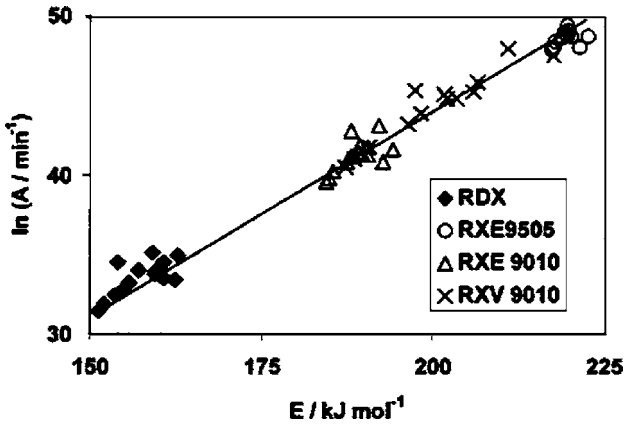

Fig. 9. The linear dependence of ln(A) with E for RDX and its PBXs obtained using conventional model fitting methods.

E_α for PBX samples is independent of α and has a value of $\sim$200 kJ mol^{-1} for all three of them. This shows that liquid phase thermolysis is the dominant process throughout their thermolysis. The role of binder is to prevent evaporation of liquid RDX and thus thermolysis proceeds in the melt phase itself. This is also supported by higher exothermic ΔH value for the PBXs.

4.2. Ignition delay measurements

Although RDX is a high explosive, it and its PBXs ignited rather than exploding. This may be due to the unconfined condition in our experimental set up. More or less same values of t_{id} and E^* were obtained for RDX and its PBXs. This shows that the mechanism of thermal ignition is same for all the samples. The reason for obtaining small value for E^* has been explained in our previous paper [11]. Thus binder does not seem to play any significant role during thermal ignition of RDX in its PBXs. However, boiling of Estane was visible during ignition delay measurements of RXE 9010.

5. Conclusions

Thermal stability of RDX is not affected by coating it with Estane or Viton A to make corresponding PBXs. The binder seems to affect the reaction pathways during thermolysis and facilitates the condensed phase processes by restricting the evaporation of molten RDX, during thermolysis. The conventional model fitting methods are constrained by kinetic compensation effect and fail to reveal the complexities of RDX decomposition. Isoconversional analysis shows that activation energy varies with extent of conversion for pure RDX, whereas it is independent of extent of conversion for the PBX samples. The initial stages of RDX thermolysis is dominated by liquid phase decomposition and the other competing channels contribute more at higher extent of conversion. Isothermal decomposition of the PBXs happens mainly in the condensed phase. Ignition delay data and its kinetic parameters show that binder does not have a significant role in thermal ignition of PBXs.

Acknowledgements

The authors are thankful to Head, Department of Chemistry, for laboratory facilities. Financial support from DRDO, New Delhi is also gratefully acknowledged. One of the authors (SPF) is grateful to CSIR, New Delhi for financial assistance. Director, TBRL, Chandigarh is thanked for the samples. Prof. G.N. Mathur, Director, Dr. D.K. Setua, Mr. Amitabh Chakaborthy and Mr. Y.N. Gupta all of DMSRDE, Kanpur are also thanked for TG-DTG and DSC data.

References

[1] C.B. Storm, J.R. Stine, J.F. Kramer, Sensitivity Relationship in Energetic Materials in Chemistry and Physics of Energetic Materials, Kluwer Academic Publishers, Dordrecht, 1990.
[2] Y. Oyumi, Propell. Explos. Pyrotech. 13 (1988) 42.
[3] H. Bazaki, N. Kubota, Propell. Explos. Pyrotech. 25 (2000) 312.
[4] F. Chaves, J.C. Gois, P. Simoes, Proceedings of the 27th International Pyrotech. Seminar, 2000, p. 865.
[5] M.S. Campbell, D. Garcia, D. Idar, Thermochim. Acta 357–358 (2000) 89.
[6] A.S. Tompa, R.F. Boswell, Thermochim. Acta 357–358 (2000) 169.
[7] M. Lal, S.R. Nayak, R. Narang, S.N. Singh, J. Armt. Stud. XXVII (2) (1992) 142.
[8] J.S. Lee, C.K. Hsu, Proceedings of the 28th NATAS Annual Conference on Thermal Analysis and Applications, 2000, p. 383.
[9] M.J. Metzger, S.M. Nicolich, D.A. Geiss, R.L. Hatch, K.E. Lee, Proceedings of the 30th International Annual Conference of ICT, 1999, pp. 4/1-4–4/14.
[10] G. Singh, S.P. Felix, Proceedings of the Fifth Seminar on New Trends in Research of Energetic Materials, 2002, p. 68.
[11] G. Singh, S.P. Felix, P. Soni, Thermochim. Acta 399 (2003) 153.
[12] M.A. Cook, G.S. Horsley, W.S. Patridge, W.O. Ursenbach, J. Chem. Phys. 24 (1956) 60.
[13] M.A. Cook, E.B. Mayfield, W.S. Patridge, J. Chem. Phys. 59 (1975) 675.
[14] S. Zeman, Thermochim. Acta 49 (1981) 219.
[15] S. Zeman, M. Dimur, S. Truchilk, Thermochim. Acta 78 (1984) 181.
[16] S. Zeman, Thermochim. Acta 41 (1980) 199.
[17] S. Zeman, Thermochim. Acta 31 (1979) 269.
[18] D.A. Frank-Kamenetskii, Acta Physiochem. USSR 10 (1939) 365.
[19] M.E. Brown, D. Dollimore, A.K. Galwey, Reactions in Solid State, Comprehensive Chemical Kinetics, Elsevier, Amsterdam, 1980.
[20] J. Sestak, Thermophysical properties of solids Comprehensive Analytical Chemistry, vol. 12D, Elsevier, Amsterdam, 1984.
[21] S. Vyazovkin, C.A. Wight, J. Phys. Chem. A 101 (1997) 8279.
[22] S. Vyazovkin, C.A. Wight, Int. Rev. Phys. Chem. 17 (1998) 407.
[23] M.E. Brown, M. Maciejewski, S. Vyazovkin, R. Nomen, J. Sempere, A. Burnham, J. Opfermann, R. Strey, H.L. Anderson, A. Kemler, R. Keuleers, J. Janssens, H.O. Desseyn, C.R. Li, T.B. Tang, B. Roduit, J. Malek, T. Mitsuashi, Thermochim. Acta 355 (2000) 125.
[24] S. Vyazovkin, C.A. Wight, Annu. Rev. Phys. Chem. 340–341 (1997) 53.
[25] S. Vyazovkin, Thermochim. Acta 355 (2000) 155.
[26] G. Singh, R.R. Singh, Res. Ind. 23 (1978) 92.
[27] G. Singh, I.P.S. Kapoor, S.K. Vasudeva, Indian J. Technol. 29 (1991) 589.
[28] G. Singh, I.P.S. Kapoor, J. Phys. Chem. 96 (1992) 1215.
[29] R. Meyer, Explosives, 3rd ed., VCH, Weiheim, Germany, 1987.
[30] N. Semenov, Chemical Kinetics and Chemical Reactions, Clarendon Press, Oxford, 1935, Chapter 2.
[31] E.S. Freeman, S. Gordon, J. Phys. Chem. 60 (1956) 867.
[32] J. Zinn, R.N. Rogers, J. Phys. Chem. 66 (1962) 2646.
[33] K. Kishore, Propell. Explos. 2 (1977) 78.
[34] G.T. Long, S. Vyazovkin, B.A. Breams, C.A. Wight, J. Phys. Chem. B 104 (2000) 2570.
[35] R.N. Rogers, L.C. Smith, Thermochim. Acta 1 (1970) 1.
[36] R.N. Rogers, Thermochim Acta 9 (1974) 444.
[37] F.C. Rauch, A.J. Fanelli, J. Phys. Chem. 73 (1969) 1604.
[38] M.A. Schreoder, Proceedings of the 17th Jannaf Combust. Meeting, 329, vol. II, CPIA Publications, 1980, p. 493.
[39] T.B. Brill, P.E. Gongwer, G.K. Williams, J. Phys. Chem. 98 (1994) 12242.